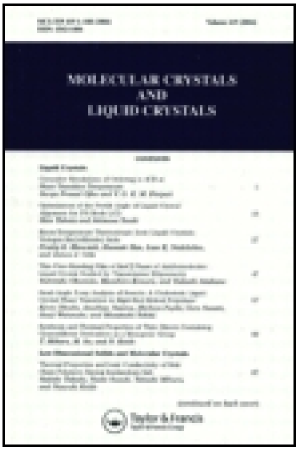

Molecular Crystals and Liquid Crystals Incorporating Nonlinear Optics
Publication details, including instructions for authors and subscription information:
http://www.tandfonline.com/loi/gmcl17

Infinite Periodic Minimal Surfaces: A Model for Blue Phases

E. Dubois-violette [a], B. Pansu [a] & P. Pieranski [a]
[a] Laboratoire de Physique des Solides, associé au C. N. R. S., Bắt. 510, Universite de Paris-Sud Centre d'Orsay, F91405, Orsay
Version of record first published: 22 Sep 2006.

To cite this article: E. Dubois-violette, B. Pansu & P. Pieranski (1990): Infinite Periodic Minimal Surfaces: A Model for Blue Phases, Molecular Crystals and Liquid Crystals Incorporating Nonlinear Optics, 192:1, 221-237

To link to this article: http://dx.doi.org/10.1080/00268949008035634

Mol. Cryst. Liq. Cryst. 1990, Vol. 192, pp. 221–237
Reprints available directly from the publisher
Photocopying permitted by license only

Printed in the United States of America

Infinite Periodic Minimal Surfaces: A Model for Blue Phases

E. DUBOIS-VIOLETTE, B. PANSU, P. PIERANSKI

Laboratoire de Physique des Solides, associé au C. N. R. S., Bât. 510, Université de Paris-Sud, Centre d'Orsay, F91405 Orsay

(*Received December 14, 1989*)

The local constraint of double twist cannot lead to long range order in our physical space $\mathbb{R}^3$. Cubic blue phases can be interpreted as an array of disclination lines. The symmetry I432, $P4_232$ and $I4_132$ of cubic blue phases can be deduced from the symmetry groups of the P, F and G infinite periodic minimal surfaces by removing all the mirror operations incompatible with chirality. Axes of double twist cylinders are shown to be the same as the core of the labyrinths of infinite periodic minimal surface. The blue phase configuration is then driven by boundary conditions on the axes of double twist cylinders and on the minimal surface. We show that the configuration which minimizes the elastic free energy on the minimal surfaces is defined by the asymptotic lines.

1. INTRODUCTION

Liquid crystalline blue phases are observed in a very narrow range of temperature between the cholesteric and isotropic phases. They present Bragg reflections in visible light. Two phases BP I and BP II are cubic phases with respective space groups $I4_132$ and $P4_232$. Investigation of the very nature of the crystalline order suggests they are crystals (periodic network) of disclinations. The presence of disclinations is a typical feature of systems where geometrical frustration does occur. This frustration results from the fact that a local constraint (absolute minimization of the free energy) defining the local order does not lead to long range order. Two different approaches can be used to describe these frustrated crystals. A first one consists in generating perfect ordered phases but in a curved manifold. Then in order to come back to reality (our physical space $\mathbb{R}^3$) one needs to decurve the space. Decurving the space is a process where typically disclinations are introduced. The second approach is a kind of compromise: one tries to realize, as best as possible in $\mathbb{R}^3$, local order compatible with a long range one. In this process defects are ab initio present and local order is only a "quasi perfect" one. The aim of this paper is to present briefly how these two descriptions suggest that the cubic blue phases are linked to infinite periodic minimal surfaces (IPMS in the following).

In the first approach, considerations on decurving process establish a simple link with some polyhedrical surface topologically equivalent to one IPMS. In the second approach similarities between blue phases and lyotropic systems are emphasized. We show that axes of double twist cylinders have the same configurations as the core of the labyrinths of lyotropic phases. These are also the core of the IPMS. The blue phase is then seen as having a double set of boundary conditions, one on the axes of double twist cylinders and the other on the IPMS. The presentation will be cursory in place when it will correspond to arguments already developed in details in other references. In the last part of this paper we look for boundary conditions on the IPMS which minimize the elastic free energy.

2. PERFECT ORDERED BLUE PHASE

We just want to sketch briefly the very nature of the perfect order on the curved space S^3. A detailed presentation has been given in Reference.[1,4] The blue phase can be described with a uniaxial order parameter $\underset{\sim}{n} \sim -\underset{\sim}{n}$ and the local order is driven by the absolute minimization condition of the free energy which reads:

$$\partial_i n^j + q_0 \, \epsilon_{ikl} \, \delta^{jk} \, n^l = 0 \qquad (1)$$

This is the famous double twist rule which leads to a frustrated phase in $\mathbb{R}^3$ (no long range order can be generated by satisfying this rule step by step) as indicated in Figure 1. In other words, in $\mathbb{R}^3$ it does not exist any configuration (director field $\underset{\sim}{n}(\underset{\sim}{r})$) satisfying the double twist rule of Equation 1. On the contrary such a texture does exist in S^3 (hypersphere embedded in $\mathbb{R}^4$). The corresponding director field is easily described in terms of a "Hopf foliation".[4] In order to visualize objects on S^3 and more precisely director field lines we use a stereographic projection. We are aware of how the classical sphere S^2 is stereographically projected on $\mathbb{R}^2$. In a

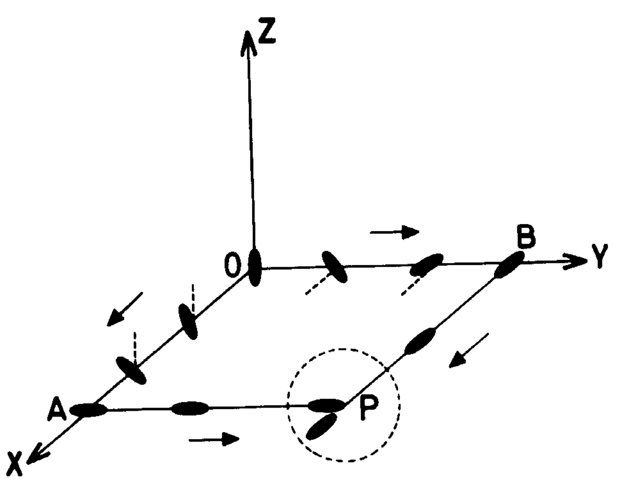

FIGURE 1 Frustration. Following the double twist rule step by step from 0 to P along OBP or OAP leads to two different orientations of the molecules at point P.

similar way the hypersphere can be projected on $\mathbb{R}^3$. A striking feature is that S^3 can be covered by a series of "parallel" tori (= nested in one another) as revealed by the stereographic projection of Figure 2. Each torus can itself be covered by a series of non interesecting great circles (Figure 3). The director field satisfying the double twist rule in S^3 is generated by this series of great circles as illustrated in Figure 4. Let us notice that in a crude way these tori may appear as a closure of double twist cylinders presented in Section 4.

3. HYPERBOLIC PLANE AND IPMS

In order to establish one of the links between the blue phases and the IPMS, we want to situate what is involved when a disclination is introduced in the perfect phase. It is worth pointing out that tori on S^3 which have a zero intrinsic curvature $\mathcal{R}$ can be seen as resulting from a transformation on squares. The transformation is indicated in Figure 5 where a square is first transformed into a cylinder and then into a torus. Let us emphasize that the torus which is generated lives in S^3. It is different from a doughnut (or a tire) which cannot be generated by closing a cylinder without stretching or tearing. Such a doughnut would get a non constant (inhomogeneous) intrinsic curvature. We have seen that director field lines of S^3 blue phases are great circles on the tori. Fathers of such lines in the above transformation are lines parallel to the diagonal of the initial square. As shown in details in Reference 4 the introduction of a disclination of strength $-\frac{1}{2}$ transforms one torus into a disclinated torus with three lobes and with the corresponding disclinated field lines. The disclinated torus can be topologically[3] built, with use of a Volterra process (= introduction of half a space) at step b of the transformation indicated in Figure 5. After the introduction of half a cylinder (Figure 6b) we close the resulting configuration and obtain the torus with three lobes (Figure 6c). Disclinated director field lines have been analytically described in Reference 4. But we can also recover their trajectories with use of the transformation.

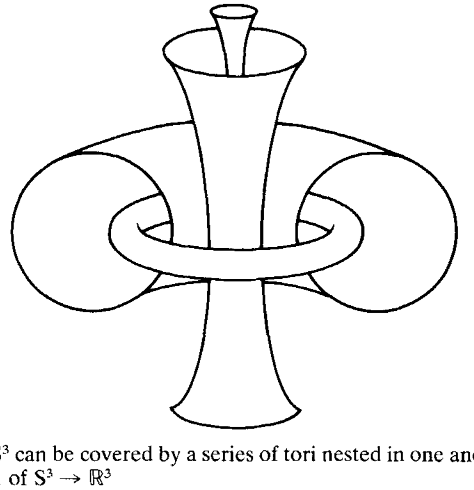

FIGURE 2 The sphere S^3 can be covered by a series of tori nested in one another. The drawing shows a stereographic projection of $S^3 \to \mathbb{R}^3$

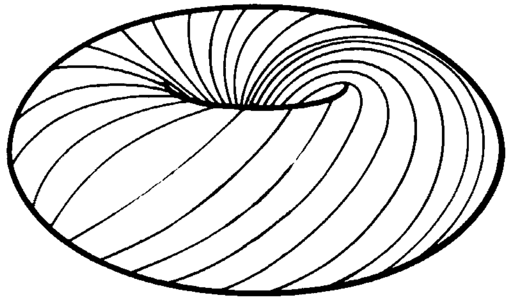

FIGURE 3 Director field lines on one torus, it is directed along great circles covering the torus.

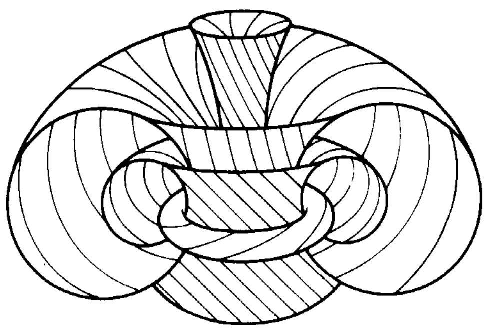

FIGURE 4 Director field lines on the series of tori covering S^3 and performing double twist.

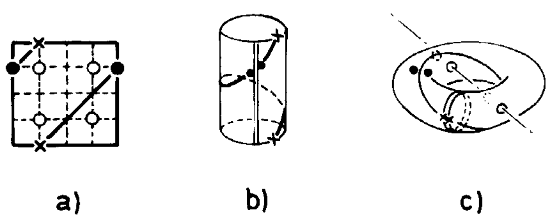

FIGURE 5 Director field lines on one torus; c) may be seen as resulting from a transformation on a square (a). First we identify the two sides of a square and obtain a cylinder. Then a second identification on the two limiting circles leads to the torus. Fathers of great circles on the torus are lines parallel to the diagonal of the initial square. ○ indicates where the disclination goes through the surface.

To follow the metamorphosis of a director field line under this process, we tile the initial square with smaller squares (doted lines in Figure 5a) such that the director field line is directed along the diagonals of the small squares. First notice that the introduction of a disclination in the center of a square transforms it into a non planar hexagon[3] (Figure 7) built with 6 squares of angles $\pi/2$ meeting at its center. Figure 7a represents ¼ of the Figure 5 where we see the four points where

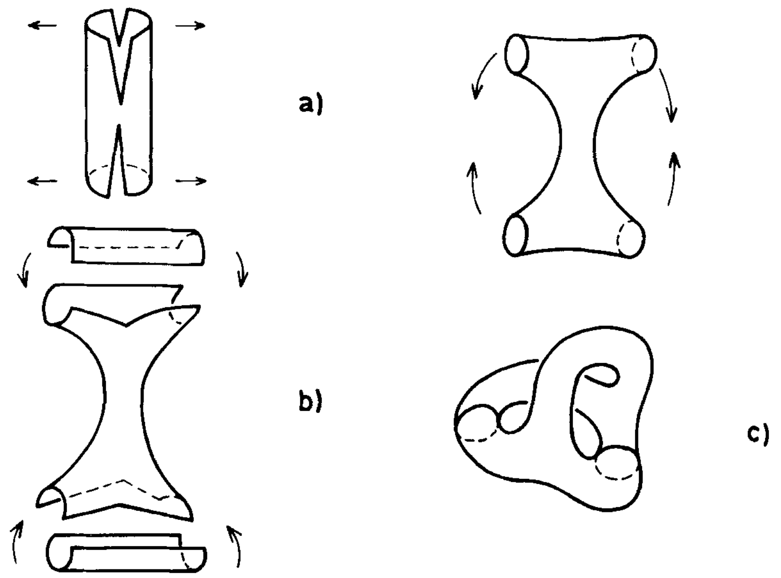

FIGURE 6 Topological construction of a disclinated torus; (a) Half a cylinder is added to one cylinder of Figure 5b (Volterra process). The closure of the obtained configuration (b) leads to the disclinated torus c).

the disclination goes through the surface. The global configuration created by the introduction of a disclination is shown in Figure 8a where sides which are identified are labelled with the corresponding numbers i.e. (1, 1'), (2, 2') and so on. We also see the corresponding director field line directed along diagonals of the squares. It starts from point 1 and follows the diagonals of the squares, arriving at point 2 it jumps to the identified point 2' and moves on the next diagonal 2'3 and so on. After the closure of Figure 8a we obtain the torus with three lobes (Figure 8b) and the resulting trajectory of the director field line is obtained in a simple way. Figure 8a is divided into three zones which are also seen in Figure 8b. Moving from point 1 → point 2 it moves from zone 1 to zone 2, then travels in zone 2 (point 2 → point 2'). Moving from point 2' to point 3, it moves from zone 2 → zone 3. It remains in zone 3 (points 3, 4, 4') and then from point 4' → point 5 it changes

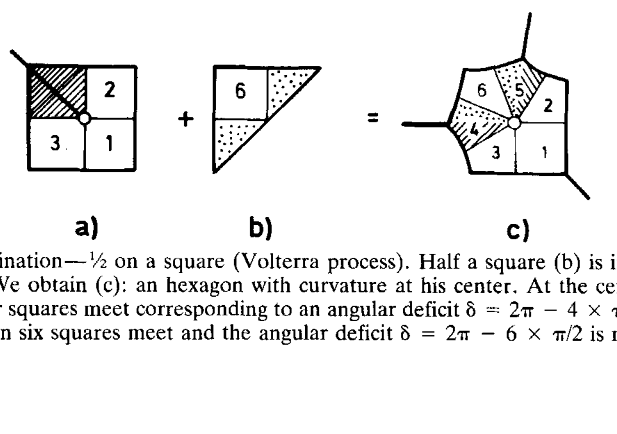

FIGURE 7 Disclination—½ on a square (Volterra process). Half a square (b) is introduced on the intial square (a). We obtain (c): an hexagon with curvature at his center. At the center of the initial square four smaller squares meet corresponding to an angular deficit $\delta = 2\pi - 4 \times \pi/2$. At the center of the final hexagon six squares meet and the angular deficit $\delta = 2\pi - 6 \times \pi/2$ is negative.

a)

b)

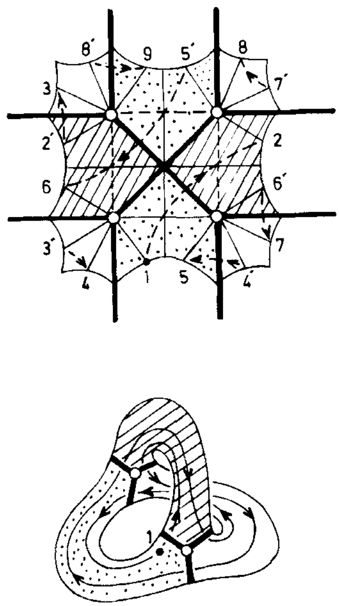

FIGURE 8 Director field lines on a disclinated torus; a) Introduction of a disclination, with the Volterra process described in Figure 7, on the initial configuration of the director field lines (Figure 5a). The director field lines are directed along the diagonals of the squares. Points labelled with the same numbers (i, i') are identified in order to obtain the closed configuration (b); in (b) we recognize the three zones , , of (a) swept by the director field lines.

again of zone (zone 3 → zone 1). In this way we reproduce the trajectory obtained analytically in Reference 2, where the director field line sweeps each lobe two times (in two opposite directions).

Let us now emphasize what happens, from the point of view of the curvature, when a disclination is inserted. The introduction of the disclination adds to the initial square (Figure 7a) (with 4 smaller squares) half a square (with 2 smaller one). This gives a final hexagon with 6 smaller squares. The resulting hexagon has curvature at its center which can be estimated from the angular deficit. We recover that the initial square is flat since at its center we get four smaller squares, the angular deficit $\delta = 2\pi - 4 \times \pi/2 = 0$. On the contrary at the center of the hexagon where six smaller squares meet the angular deficit is $\delta = 2\pi - 6 \times \pi/2 = -\pi$. This emphasizes that the introduction of the disclination $S = -1/2$ implies the introduction of negative curvature. If the curvature was uniformly spread one would obtain a surface with constant negative curvature such as the hyperbolic plane H_p. The hyperbolic plane is not embedded in our physical space $\mathbb{R}^3$, only part of it can be. Nevertheless there is some interest to look at what could be the blue phase director field on the hyperbolic plane. Indeed what we would like to obtain is an intermediate unflattening leading to a surface leaving in $\mathbb{R}^3$. Every introduction of a disclination $S = -1/2$ at one point of the torus leads to a new surface with negative curvature at this point. The introduction of a finite number of disclinations would lead to a surface with negative curvature at points where the disclinations are introduced and flat elsewhere.

Having in mind that the final state we want to obtain must be a cubic periodic one a good example of such an organization is seen on the polyhedron (Figure 9) which is topologically equivalent to the P IPMS,[5] where we recognize, hexagons constituted of 6 squares. Such organization presents a periodic repartition of disclinations in the directions [111] of the cubic array. On the polyhedral surface the curvature is localized on the vertices of the cubic array; at each vertex there is the same negative density of curvature. In the IPMS the curvature is always negative and spread all over the surface. It is not homogeneous. The hyperbolic plane corresponds to an homogeneous repartition of negative curvature. The IPMS appears as having an intermediate repartition of curvature between the one of the polyhedral surface and the one of the hyperbolic plane. The polyhedral surface is not a smooth surface and the corresponding director field built on it will present brutal changes. Nevertheless since it is topologically equivalent to the P surface, it is of interest to consider the director field on it since it can be generated in an easy way as the parallels to the diagonals of the squares (Figure 10). Three director lines meet at the center of the Figure 10 where the disclination (along the [111] direction) goes through the surface. It has been shown[8] that one can establish a correspondence between the hyperbolic plane and the IPMS. This correspondence is realized if some translations of the hyperbolic plane are tranformed into identifications. This relates the fundamental region (Figure 11) of the hyperbolic plane to the cell (Figure 10) of the P surface. Director field lines can also be generated on the hyperbolic plane as the diagonals of the squares of the {4,6} tiling. In Figure 11 we see the fundamental region with 6 full squares and 12 half squares corresponding to the cell of the polyhedron of Figure 10. Points A, B, C . . . on the hyperbolic plane (Figure 11) are identified in order to constitute the channels of the polyhedron (Figure 10).

As a conclusion of this section we have seen that the director field lines which are great circles on tori of S^3 can be seen as diagonals of a square tiling. Then the

(a)

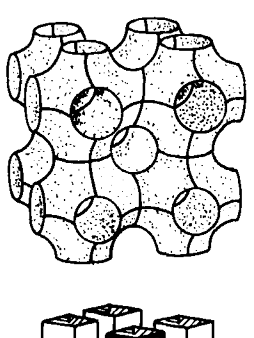

(b)

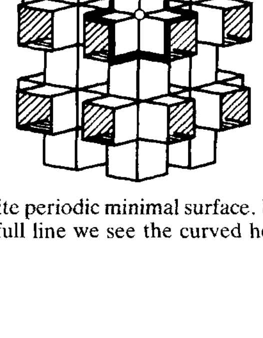

FIGURE 9 a) The P Schwarz infinite periodic minimal surface. b) The polyhedral surface topologically equivalent to the P surface. In big full line we see the curved hexagon formed by 6 squares.

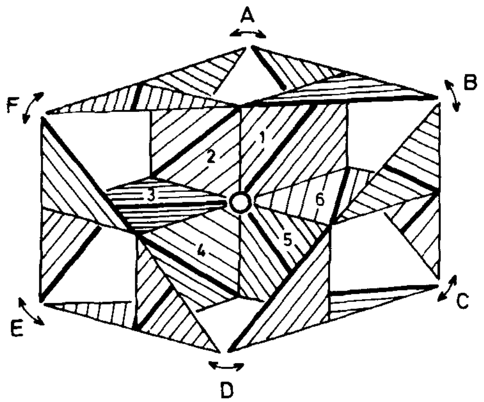

FIGURE 10 Polyhedral surface with the corresponding director field lines parallel to the diagonal of the squares. Bigger lines show singular director field lines.

introduction of disclinations (space decurving) transforms the initial surface in surfaces with negative curvature. The director field line is still generated by diagonals of the corresponding square tiling and presents singularities at the points where disclinations go through the surface. Arguments involving the decurving of the space have led to consider IPMS as good candidates to describe blue phases. We shall now see that symmetry arguments, based on models in $\mathbb{R}^3$, reinforce this conclusion.

4. DOUBLE TWIST CYLINDERS AND IPMS

The alternative description concerns models[9,10] in $\mathbb{R}^3$ where the notion of double twist cylinders is introduced. The constraint of Equation 1 is mostly satisfied in finite regions of the space called double twist cylinders as shown in Figure 12. The tilt of the molecules is more and more pronounced when moving away from the

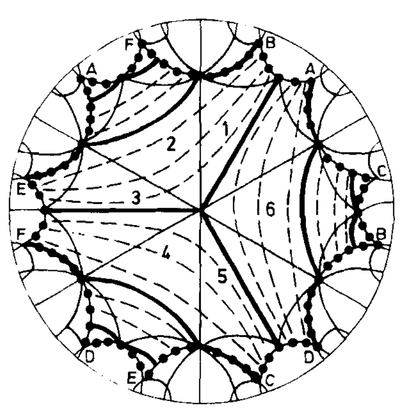

FIGURE 11 Tiling {4, 6} of the hyperbolic plane (Poincaré representation). Dotted lines delimit the fundamental region where points labelled by the same letters are identified in order to build channels of the polyhedral surface of Figure 10. Bigger lines correspond to singular director field lines.

cylinder axis. The condition 1 is only satisfied in the limit of r → 0 (r = radial distance from the axis). The next step in these models is to find a periodic arrangement of these tubes (of finite size) such that its space group corresponds to the one of the cubic blue phases observed experimentally. Blue phase I(O^8) and blue phase II(O^2) corresponds respectively to space groups I $4_1 32$ and P $4_2 32$. A last model[11] (O^5), not confirmed by experimental results, but of theoretical interest corresponds to the space group I 432. Cubic phases in lyotropic systems are also concerned with the space groups Ia3d = I4_1/a $\bar{3}$ 2/d and Pn3m = P4_2/n $\bar{3}$ 2/m. The space group Im3m = I 4/m $\bar{3}$ 2/m is not frequently observed except in some exotic systems such as etiolated Avena leaves[13]. It is worth pointing out that space groups of the blue phases correspond to the last ones if mirror operations, incompatible with the chirality of the molecules, are taken off. These groups are also those of the three cubic IPMS refered as the P, F and G surfaces.[5,6] Axes of double twist cylinders in the O^5, O^2 and O^8 blue phase structures correspond to the core of the labyrinths of the P, F and G IPMS. This link is trivial for the O^5 structure (Figure 12). For the O^2 and O^8 structures[9,10] the initial stacking of double twist cylinders is not directed along the core of the F and G surfaces. But it is shown[12] that, associated with the initial stacking of double twist cylinders, there exist new double twist cylinders whose axes correspond to the core of the labyrinths of the P, F and G IPMS. This skeleton reveals two infinite networks, unconnected but mutually interwoven that we label 1 and 2 for simplicity as in Figure 12 for the P surface. In models of References 9 and 10 the double twist tubes are of finite extension. Here in our model we let the double twist tubes swell in order to fill all the space (Figure 12). Due to the above arguments and the one developed in the preceding section it is reasonable to assume that the surface of separation between the two networks of swollen double twist tubes is the corresponding minimal surface. What we now want to determine is the configuration of the director field lines on this surface.

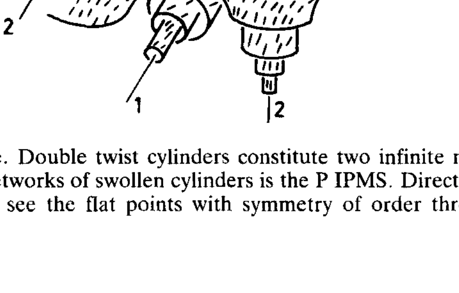

FIGURE 12 O^5 structure. Double twist cylinders constitute two infinite networks (1) and (2). The surface between the two networks of swollen cylinders is the P IPMS. Director field lines are along the asymptotic directions. We see the flat points with symmetry of order three where disclinations go through the surface.

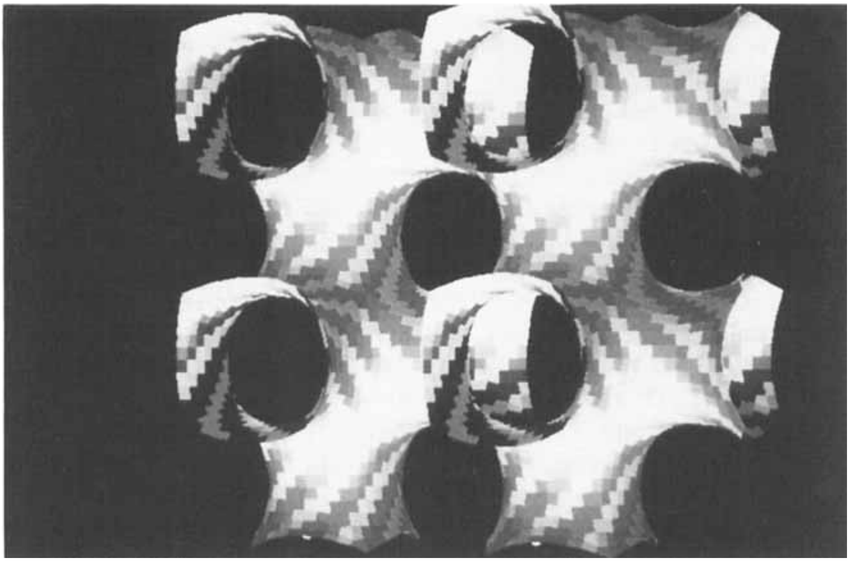

Photo 1. The P IPMS and director field lines

5. DIRECTOR FIELD LINES ON THE IPMS

In order to determine the blue phase configuration on the IPMS we need two ingredients. First a description of the IPMS and then a calculation of the free surface energy. A parametrization of the IPMS is obtained with use of two maps.

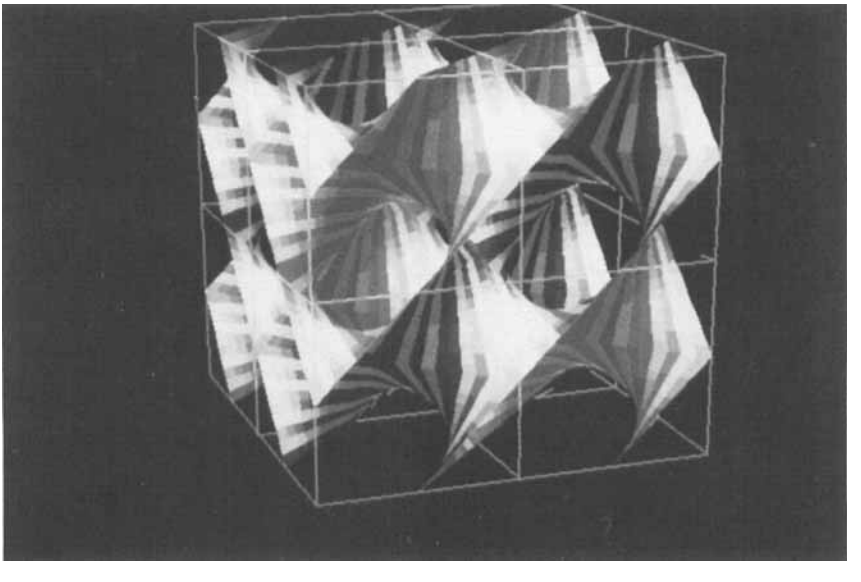

Photo 2. The F IPMS and director field lines

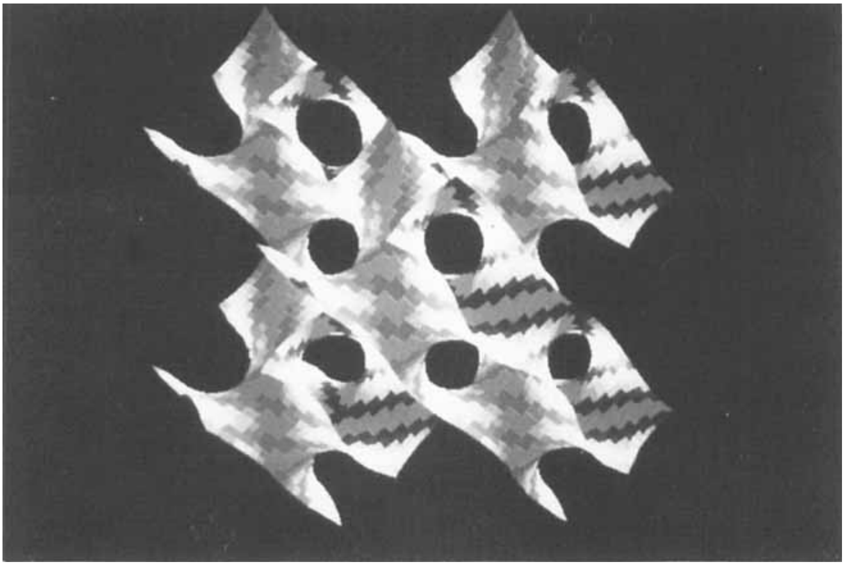

Photo 3 The G IPMS and director field lines

First the Gaussian map relates each point of the surface x^i (i = 1, 2, 3) to a point of the unit sphere representing the normal $\underset{\sim}{N}(\underset{\sim}{x})$ to the surface. Then a stereographic projection gives a map onto the complex plane (Figure 13)

$$P\,(x^i) \xrightarrow{g} N^i \xrightarrow{s} \omega = \sigma + i\tau$$

$$\text{IPMS} \qquad S^2 \qquad \mathbb{R}^2$$

The Weierstrass's integral representation of the IPMS is expressed in terms of an holomorphic function R(ω) of ω depending on the flat points[7] (points with zero Gaussian curvature) of the minimal surface. A point of the IPMS is defined by the coordinates:

$$x_i = \frac{\gamma}{2}\left\{\int a^i(\omega)\, R(\omega)\, d\omega + c.c\right\} \tag{2}$$

where γ is a constant and c.c means complex conjugate. The three complex functions $a^i(\omega)$ are given by:

$$\begin{cases} a^1(\omega) = 1 - \omega^2 \\ a^2(\omega) = i(1 + \omega^2) \\ a^3(\omega) = -2\omega \end{cases} \tag{3}$$

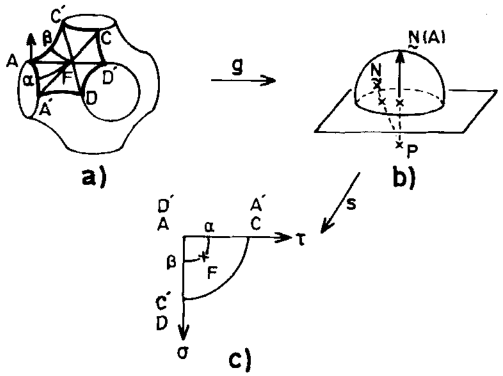

FIGURE 13 Weierstrass's representation of the IPMS in terms of $\omega = \sigma + i\tau$. The surface is first map onto its spherical image: point A $\rightarrow$ normal $\underset{\sim}{N}(A)$ and then on a plane via the stereographic projection, from south pole P, $\underset{\sim}{N}(A) \rightarrow \omega_A$. The circuit shown in a) covers twice the circuit indicated on c). Corresponding points are labelled by the same letters. Trajectories βF and αF are circles (centers $\sigma = -1, \tau = -1$, radius $\rho = \sqrt{2} - 1$). CC' is a circle (center A, radius $\rho = 1$).

and the relations:

$$\begin{aligned}
&\sum_i a^i N^i = 0 \\
&\sum_i (a^i)^2 = 0 \\
&\sum_i a^i \bar{a}^i = 2(1 + \omega\bar{\omega})^2 \\
&\sum_i a^i \, d\bar{a}^i = 4(1 + \omega\bar{\omega})\omega d\bar{\omega}
\end{aligned} \tag{4}$$

will be useful in the following.

For the P, F and G IPMS the holomorphic function is[7]:

$$R(\omega) = \prod_{k=1}^{8} 1/(\omega - \omega_k)^{1/2},$$

where $\omega_k = N_k^1/(1 + N_k^3) + iN_k^2/(1 + N_k^3)$, $\underset{\sim}{N}_k$ being the external normal at the k[th] flat point. The value ω_k at the 8 flat points are:

$$\omega = \pm\,\alpha(1 \pm i)$$

$$\omega = \pm\,\beta(1 \pm i)$$

with $\alpha = \sqrt{3}/(\sqrt{3} - 1)$ and $\beta = \sqrt{3}/(\sqrt{3} + 1)$

which leads for the P surface to:

$$R_p(\omega) = (1 + 14\omega^4 + \omega^8)^{-1/2}.$$

$R_p(\omega)$ which is a holomorphic function of ω can be written as:

$$R_p(\omega) = r(\omega,\bar{\omega})\, e^{i\theta(\omega,\bar{\omega})}$$

$r(\omega,\bar{\omega})$ is the norm of $R_p(\omega)$, $\theta(\omega,\bar{\omega})$ its argument is harmonic.

The three surfaces P, F and G are associated surfaces i.e. they are related by a Bonnet transformation. In this transformation only bent is involved; there is no stretching and no tearing. It preserves lengths, angles and surfaces. The intrinsic curvature is preserved. They can be transformed one into the other just by adding a constant phase θ_0 to $\theta(\omega,\bar{\omega})$. The F and G surface are deduced from the P one by adding the respective phases:

$$\theta_F = \pi/2$$

$$\theta_G \approx 38°.$$

The lengths on the surfaces are related to the metric tensor. The frame, associated to the coordinates (σ,τ) defined by $\omega = \sigma + i\tau$, is orthogonal since any arc length can be expressed as:

$$dl^2 = \sum_i (dx^i)^2 = t^2(d\sigma^2 + d\tau^2) \tag{5}$$

with:

$$t(\omega) = \gamma r(\omega,\bar{\omega})(1 + \omega\bar{\omega}) \tag{6}$$

This length only depends on $r(\omega, \bar{\omega})$ and is therefore the same for all the associate surfaces. The curvature tensor is deduced from the first and second fundamental form. F_1 is determined from Equation 5:

$$F_1 = \gamma^2\, r^2(\omega, \bar{\omega})(1 + \omega\bar{\omega})^2 \begin{bmatrix} 1 & 0 \\ 0 & 1 \end{bmatrix}$$

The second fundamental form results from the computation of $\langle \delta N . \delta P \rangle$ with use of Equation 2 and of the following relations:

$$N^1 = (\omega + \bar{\omega})/(1 + \omega\bar{\omega})$$

$$N^2 = i(\bar{\omega} - \omega)/(1 + \omega\bar{\omega}) \tag{7}$$

$$N^3 = (1 - \omega\bar{\omega})/(1 + \omega\bar{\omega})$$

which give:

$$dN^i = (\bar{a}^i\, d\bar{\omega} + c.c)/(1 + \omega\bar{\omega})^2.$$

We obtain:

$$\langle \delta N.\delta P \rangle = 2\gamma r(\omega, \bar{\omega})\, [\cos\theta(d\sigma^2 - d\tau^2) - 2\sin\theta\, d\sigma\, d\tau]$$

and

$$F_2 = 2\gamma r(\omega, \bar{\omega}) \begin{bmatrix} \cos\theta & -\sin\theta \\ -\sin\theta & \cos\theta \end{bmatrix}$$

The curvature tensor $\mathcal{R} = F_2/F_1$ simply reads:

$$\mathcal{R} = \left[2/[\gamma r(\omega, \bar{\omega})\,(1 + \omega\bar{\omega})^2]\right] \begin{bmatrix} \cos\theta & -\sin\theta \\ -\sin\theta & -\cos\theta \end{bmatrix} \tag{8}$$

The mean curvature is the trace of this tensor and is zero which is characteristic of a minimal surface. The Gauss curvature $\mathcal{C}_G$ is equal to the determinant of this tensor, it is then negative and only depends on ω and $r(\omega, \bar{\omega})$. As a consequence all associate minimal surfaces have the same distribution of Gauss curvature. The argument function $\theta(\omega, \bar{\omega})$, which changes by a constant term from one minimal surface to an associate one, defines the orientation of the principal directions in the natural frame (σ, τ). At each point of the surface, each tangent direction defines with the normal a normal plane and a curve on the surface with a specific curvature k. There exists one pair of orthogonal directions for which this curvature k is extremum: they are the principal directions. Their orientations are defined by an angle μ_p in the natural frame (σ, τ) and are obtained by diagonalization of the matrix $\mathcal{R}$(Equation 8). The two principal directions are defined by:

$$\begin{aligned} \mu_P &= -\theta/2 \\ \mu_{P'} &= -\theta/2 + \pi/2. \end{aligned} \tag{9}$$

They correspond to the curvature $k_P = 2/(\gamma\, r(\omega, \bar{\omega})(1 + \omega\,\bar{\omega})^2)$ and $k_{P'} = -k_P$. The directions along which k is zero are called asymptotic directions. At each point of the minimal surface, there exists a pair of such directions which lie at $\pi/4$ from the principal directions. They correspond to:

$$\begin{aligned} \mu_A &= -\theta/2 + \pi/4 \\ \mu_{A'} &= -\theta/2 + 3\pi/4. \end{aligned} \tag{10}$$

Let us notice that when straight lines lie on the minimal surface they are necessarily along some asymptotic directions. From relations (9) and (10) we conclude that for the adjoint surfaces F and P (phase shift $\theta_0 = \pi/2$) the asymptotic or principal directions of one surface correspond respectively to the principal or asymptotic directions of the other one.

ENERGY

We now want to determine what is the precise configuration of the director on the IPMS which will be further on considered as a boundary condition. The free energy is:

$$F = \int \mathcal{F} \mathrm{vol}$$

where:

$$\begin{aligned} 2\mathcal{F} = {} & K_{11}(\mathrm{div}\ \underset{\sim}{n})^2 + K_{22}(\underset{\sim}{n}.\mathrm{curl}\underset{\sim}{n} + q_0)^2 + K_{33}(\underset{\sim}{n}.\mathrm{curl}\underset{\sim}{n})^2 \\ & - (K_{22} + K_{24})\ \mathrm{div}\ (\underset{\sim}{n}.\mathrm{curl}\underset{\sim}{n} + \underset{\sim}{n}\mathrm{div}\underset{\sim}{n}) \end{aligned} \tag{11}$$

where q_0^{-1} is the pitch of the cholesteric.

If the elastic constants are estimated at second order in the local order parameter we get:

$$K_{11} = K_{33} = K_{24} = 0.$$

Expression (11) can be expressed easily in the one elastic constant limit $K_{11} = K_{22} = K$ as:

$$\mathcal{F} = K \sum_{k,j} [(\partial_k n^j + q_0\, \epsilon_{kji}\, n^i)^2 - q_0^2]$$

or if we introduce the double twist connection[1]

$$\nabla_i n^j = \partial_i n^j + q_0\, \delta^{jl}\, \delta_{ilp}\, n^p \tag{12}$$

$$F = \int [\nabla_i n]^j\, [\nabla_k n]^l\, g^{ik}\, g_{jl}\ \mathrm{vol}. \tag{13}$$

This energy takes into account gradient terms tangent and normal to the surface. Since we are looking at the IPMS as a boundary condition we only take into account part of the energy contained in the surface i.e. we neglect gradient terms normal to the surface. Due to symmetry considerations the director field on the surface could be either tangent or normal to it. Arguments developed in the previous sections suggest to consider a field tangent to the surface as in the polyhedral surface and which will lead to disclinations in the perpendicular direction as in models of References 9,10,11.

$$F = \sum_{k=1,2,3} \int \{[(\nabla_\sigma n)^k]^2 + [(\nabla_\tau n)^k]^2\} \, dS \tag{14}$$

where $dS = t^2 \, d\sigma \, d\tau$ and t is given by Equation 6.

The director field is defined on the surface by an angle μ with the natural frame $e_\sigma = \partial/\partial\sigma$ and $e_\tau = \partial/\partial\tau$ as:

$$\underset{\sim}{n}(\omega) = \cos \mu(\omega, \bar{\omega}) \, \underset{\sim}{e}_\sigma + \sin \mu(\omega, \bar{\omega}) \, \underset{\sim}{e}_\tau.$$

As shown in Reference 14 minimization of the energy F implies the condition:

$$\frac{\partial^2(\mu + \theta)}{\partial\omega \, \partial\bar{\omega}} + \frac{\partial^2(\mu + \theta)}{\partial\bar{\omega} \, \partial\omega} = -8q_0 \, \gamma r(\omega, \bar{\omega}) \cos(2\mu + \theta),$$

which leads to the solutions:

$$\mu = -\theta/2 + \pi/4 \; (+k\pi)$$

$$\mu' = -\theta/2 + 3\pi/4 \; (+k\pi).$$

These values correspond to the one defining the asymptotic direction (Equation 10). An array of such asymptotic lines is shown in Figure 12 for the P surface and on the three photographs for the P, F and G surfaces. Let us remark that there exist two kinds of such array. One would correspond to left twist and the other one to right twist. As in the polyhedron of Figure 10 we recognize singularities in the director field leading to disclinations in the [111] directions.

CONCLUSION

We have shown that the process of decurving the space, where a perfect ordered blue phase exists, leads to surfaces topologically similar to IPMS. On the other hand the analogy between models of blue phases in $\mathbb{R}^3$ and lyotropic cubic phases also suggest that IPMS are involved in the description of blue phases. Although we know that perfect double twist does not exist in $\mathbb{R}^3$ we have found a configuration of the director on the IPMS which realizes it as best as possible i.e. it corresponds to a relative minimum of the energy. Such a configuration is described with use of asymptotic lines on the surface.

Acknowledgments

We thank J. Charvolin and J. F. Sadoc for very rich discussions and suggestions. We have largely benefited from their experience on the hyperbolic plane and on the IPMS.

References

1. B. Pansu, R. Dandoloff and E. Dubois-Violette, *J. Phys. (Paris)*, **48**, 297 (1987).
2. E. Dubois-Violette and B. Pansu to appear in: "Geometry in Condensed Matter Physics" Directions in Condensed Matter Physics, World Scientific Publishing Company (1990).
3. J. F. Sadoc and J. Charvolin, *J. Phys. (Paris)*, **47**, 683 (1986).
4. B. Pansu, E. Dubois-Violette and R. Dandoloff, *J. Phys. (Paris)*, **48**, 1559 (1987).
5. A. Mackay, *Nature*, **314**, 314 (1985).
6. A. Schoen, Infinite Periodic Minimal Surfaces without Self Intersections, NASA Technical Note TD—5541 (1970).
7. S. Lidin and S. T. Hyde, *J. Phys. (Paris)*, **48**, 1585 (1987).
8. J. F. Sadoc and J. Charvolin, *Acta Cryst.*, **A 45**, 10 (1989).
9. S. Meiboom, M. Sammon and W. Brinkman, *Phys. Rev.*, **A 27**, 1 438 (1983).
10. R. Hornreich and S. Shtrikman, *Phys. Lett.*, **84A**, 20 (1981).
11. A. Saupe, *Mol. Cryst. Liq. Cryst.*, **7**, 59 (1969).
12. E. Dubois-Violette and B. Pansu, *Mol. Cryst. Liq. Cryst.*, **165**, 151 (1988).
13. B. Gunning, *Protoplasma*, **60**, 111 (1965).
14. B. Pansu and E. Dubois-Violette, *Europhys. Lett.*, **10**, 43 (1989).